MOLECULAR AND CELLULAR BIOLOGY, June 1988, p. 2523–2535
0270-7306/88/062523-13$02.00/0

Vol. 8, No. 6

Mutational Analysis of Centromere DNA from Chromosome VI of *Saccharomyces cerevisiae*

JOHANNES H. HEGEMANN,[1] JAMES H. SHERO,[2] GUILLAUME COTTAREL,[1] PETER PHILIPPSEN,[1] AND PHILIP HIETER[2]*

Institut fuer Mikrobiologie und Molekularbiologie, Justus Liebig Universitaet, 6300 Giessen, Federal Republic of Germany, and Department of Microbiology, Biocenter, University of Basel, 4056 Basel, Switzerland,[1] and Department of Molecular Biology and Genetics, Johns Hopkins University School of Medicine, 725 North Wolfe Street, Baltimore, Maryland 21205[2]

Received 9 October 1987/Accepted 8 March 1988

***Saccharomyces cerevisiae* centromeres have a characteristic 120-base-pair region consisting of three distinct centromere DNA sequence elements (CDEI, CDEII, and CDEIII). We have generated a series of 26 *CEN* mutations in vitro (including 22 point mutations, 3 insertions, and 1 deletion) and tested their effects on mitotic chromosome segregation by using a new vector system. The yeast transformation vector pYCF5 was constructed to introduce wild-type and mutant *CEN* DNAs onto large, linear chromosome fragments which are mitotically stable and nonessential. Six point mutations in CDEI show increased rates of chromosome loss events per cell division of 2- to 10-fold. Twenty mutations in CDEIII exhibit chromosome loss rates that vary from wild type (10^{-4}) to nonfunctional ($>10^{-1}$). These results directly identify nucleotides within CDEI and CDEIII that are required for the specification of a functional centromere and show that the degree of conservation of an individual base does not necessarily reflect its importance in mitotic *CEN* function.**

Since the first isolation (8) of a DNA clone containing a centromere of the yeast *Saccharomyces cerevisiae*, a major goal has been the identification of those DNA sequences that are important for the assembly of functional yeast centromeres. Potential candidates are nucleotides within a characteristic 120-base-pair (bp) DNA segment, which was found by sequence comparisons of cloned DNA from the centromere regions (*CEN* DNA) of 12 *S. cerevisiae* chromosomes (13, 19, 21, 29, 41).

Deletion analysis of *CEN3*, *CEN6*, and *CEN11* DNA has demonstrated that the presence of the 120-bp conserved sequence is necessary and sufficient for complete centromere activity in vivo (1, 17, 35, 40). Several segments of highly conserved base pairs within the *CEN* region contribute to palindromic structures (see Fig. 2A and B). The completely conserved uTCACuTG (u = purine) at the left end (CDEI) was recently shown to bind to a protein in cell extracts (3; L. Panzeri, personal communication), although there is at present no evidence that this protein binds CDEI in the centromere DNA in vivo. Deletions at the left end, including all or major parts of CDEI, lead to a substantial decrease in centromere activity (40). The right end with the highly conserved TGT$^{T}_{A}$T$^{T}_{A}$TG..TTCCGAA.....AAA (CDEIII) also binds to protein (17), and deletions at this end that remove parts of CDEIII lead to inactive centromeres (17, 35, 40). The internal part (CDEII) shows variable sequences, composed almost entirely of A and T nucleotides. Protein binding to this region can be inferred from chromatin digestion studies, since the 120 bp and adjacent sequences are resistant to DNases (1). Sequence rearrangements within the CDEII region show that modifications of length and A+T content of this element do affect centromere function but to a limited degree (4, 15, 39, 40).

A mutational analysis with the aim of defining the contributions of individual base pairs to centromere function should focus first on CDEI and CDEIII. The importance of the primary sequence of CDEIII has been demonstrated previously by analyzing a few single-base-pair changes (30, 35). For example, a C-to-T change in the central base of the CDEIII dyad completely eliminates centromere function when tested on plasmids or when placed onto an authentic yeast chromosome (30). G-to-A changes at each of two positions were reported to have no effect on centromere function (30), though a discrepancy for one of these mutations exists in the literature (35). In this report, we analyze a more-extensive group of mutations in CDEIII, including those previously described. Additionally, single-nucleotide substitutions in CDEI are reported here for the first time. The extent to which these results will contribute to our understanding of analogous structures in larger eucaryotic chromosomes is not known (42, 43).

Of critical importance to a mutational analysis of centromere function is the use of a reproducible and sensitive test system which is able to detect and quantitate minor changes in centromere function. In the assays used so far, loss of a plasmid or chromosome carrying mutated *CEN* DNA was monitored by following a scorable genetic marker and expressed as loss rate per cell division. The drastic differences in mitotic stability of autonomously replicating sequence (*ARS*) plasmids (50) with or without centromere DNA was first taken as a measure of centromere activity (8, 51, 52). This system has proven to be especially useful and convenient when plasmid loss can be monitored by color changes in colonies (18, 24). However, the assays based on plasmid loss are often insufficient as a result of the high basal level of instability of *ARS* plasmids carrying wild-type *CEN* DNA (loss rate of approximately 10^{-2} per cell division). It is therefore difficult to assess minor changes in centromere function with plasmids. Assay of the effects of mutated *CEN* DNAs after replacement of wild-type *CEN* DNA in whole chromosomes (9) leads to an improvement in sensitivity, since the basal level of chromosome loss in *S. cerevisiae* is approximately 10^{-5} (16). One problem inherent with this type of analysis is that loss of the genetic marker being

* Corresponding author.

TABLE 1. Oligonucleotides used to introduce the point mutations within CDEI and CDEIII

Oligonucleotide no.	Sequence[a] (5' to 3')	Mutations obtained
VI	d(CCGAAGATGT [A/T] [G/T] [A/T] ATAGGTTGAA)	CDEIII(23-T,24-G); CDEIII(24-G); CDEIII(24-G,25-T)
VII	d(AAGAAAAAATA [T/C/A] [T/G] TTTTGTTTTCC)	CDEIII(2-C); CDEIII(2-T); CDEIII(2-T,3-G); CDEIII(2-A,3-G)
XIV	d(TTGTTTTC [T/A/G] GAAGATGT)	CDEIII(14-T); CDEIII(14-A); CDEIII(14-G)
XV	d(TGTTTTCC [C/T/A] AAGATGTA)	CDEIII(15-C); CDEIII(15-A); CDEIII(15-T)
XVI	d(TCATCACG [C/A/G] GCTATAAA)	CDEI(7-C); CDEI(7-A); CDEI(7-G)
XVII	d(CATCACGT [C/T/A] CTATAAAA)	CDEI(8-C); CDEI(8-T); CDEI(8-A)
XVIII	d(ATAGTTTTTT [T/G] TTTCCGAA)	CDEIII(8-T); CDEIII(8-T,9-G)

[a] Nucleotides in brackets represent mixed positions, and underlined nucleotides are different from the wild-type sequence.

scored is also caused by mitotic recombination between homologous chromosomes in diploid cells. Furthermore, phenotypic lag in expression of or leakiness in selection for the genetic marker being uncovered can introduce error into estimates obtained by these methods. In the present study, we use a third type of assay in which the segregation of large, nonessential, linear chromosome fragments is followed (basal level of chromosome loss of approximately 10^{-4}). Work from a number of laboratories (18, 33, 34, 53) has shown that artificial chromosomes require two major determinants for their mitotic stability; they must be large (>100 kilobases [kb]) and linear (telomeres at each end). The artificial chromosomes used in our assay fulfill these criteria. The chromosome fragments carry the mutated *CEN* DNA close to one end, plus a short arm containing the *SUP11* gene embedded in pBR322 sequences, and a long arm containing most of the left arm of chromosome III. The chromosome fragments are not disadvantageous for the life cycle of yeast cells, and the type of DNA present can be directly verified by electrophoretic karyotyping. Additionally, the mitotic behavior is easily monitored by red pigment formation (44), as this implies loss of a marker *SUP11* gene, which suppresses an *ade2* mutation present in the transformed strain (18). Loss of *SUP11* by mitotic recombination cannot occur, because the short arm carrying *SUP11* has no counterpart in the wild-type chromosomes.

In this paper we describe the effects of 26 mutations introduced into the conserved left and right ends of *CEN6*. Loss rates per mitotic cell division were determined by fluctuation analysis (26) by using the chromosome fragment assay. For comparison, the *CEN* mutations were also analyzed when present on plasmids. The results identify DNA sequence determinants necessary or important in *cis* for centromere function and clearly show that the degree of conservation of a base pair is not necessarily a measure of its importance in mitotic *CEN* function.

MATERIALS AND METHODS

Enzymes, reactions, and media. Restriction enzymes, T4 DNA ligase, polynucleotide kinase, and DNA polymerase (Klenow fragment) were purchased from various companies and used under the conditions suggested by the supplier. DNA was labeled with ^{32}P by the random hexamer primer method (12). Bacterial transformations were carried out as previously described (10) or according to Mandel and Higa (27) with some modifications. Yeast transformations were performed as described previously (22). Plasmid DNA preparations from bacterial strains and all DNA manipulations were done according to Maniatis et al. (28) with minor modifications. Medium components were from Difco Laboratories, GIBCO Laboratories, or Sigma Chemical Co. Nonselective medium (YPD) and minimal medium for yeast were as described previously (48). Bacterial cells were grown in 2× YT medium (1.6% Tryptone, 1% yeast extract, 0.5% NaCl) or on 1% agar YT plates. Fluctuation analysis was performed by plating on minimal medium, supplemented with auxotrophic requirements as described previously (48), with the modification of limiting adenine (6 μg/ml) conditions for red or pink colony formation (18).

***Escherichia coli* and yeast strains.** The *E. coli* strains used were as follows: MM294 [*endA1 thi hsdR* Δ(*srlR-recA*)*306*] (source, M. Brennan), JM101 [*supE thi* Δ(*lac-pro*) F' *traD36 proAB lacI*^{q} *lacZ*Δ*M15*] (source, J. Messing), BMH71-18*mutS* [*thi supE* Δ(*lac-pro*) *recA galE rpsL* F' *lacI*^{q} *lacZ*Δ*M15 proA*$^+$*B*$^+$ *mutS215*::Tn*10*] (source, H. J. Fritz), and MK30-3 [Δ(*lac-pro*) *recA galE rpsL* F' *lacI*^{q} *lacZ*Δ*M15 proA*$^+$*B*$^+$] (source, H.-J. Fritz). The bacteriophage strains used were M13mp8 and M13mp9 (31) and M13mp18 and M13mp19 (36); M13mp9rev (25) was obtained from H.-J. Fritz. The *S. cerevisiae* strains used were SX1-2 (α *trp1 his3 ura3-52 gal2 gal10*) (source, R. Davis) and YNN290 (**a**/α *ura3-52*/*ura3-52 ade2-101*/*ade2-101 lys2-801*/*lys2-801* Δ*trp1-901*/Δ*trp1-901*) (18), which was used for the chromosomal fragmentation transformations. Strains were cured to [*psi*$^-$] as described previously (18).

Oligonucleotides. The oligonucleotides were synthesized by the Applied Biosystems DNA synthesizer 380B using phosphoramidite chemistry. The oligonucleotides used to create the point mutations are shown in Table 1. Additionally, an internal primer for dideoxy-sequence analysis of the CDEI mutants was synthesized with the sequence d(TAATGCTAAATACTC), called oligonucleotide XIX. This primer binds 78 bp upstream of CDEI. The sequencing primer for verifying the CDEIII mutations binds to CDEI (17). All oligonucleotides were purified as tritylated material in two steps as described earlier (17), first on a C18 disposable column and then by reversed-phase high-performance liquid chromatography on a C18 column (14). Finally, detritylation was performed. All oligonucleotides were terminally labeled with polynucleotide kinase.

Oligonucleotide-directed mutagenesis. Predefined mutations were introduced via synthetic oligonucleotide mixtures by the gapped duplex DNA approach (25) as described before (17). A 1.16-kb *Hin*dIII-*Bgl*II fragment carrying the *CEN6* DNA (41) was cloned into *Hin*dIII-*Bam*HI-cut M13mp9. Single-stranded DNA of this clone was mixed with double-stranded DNA of M13mp9rev, which was digested with *Eco*RI and *Hin*dIII. The gapped duplex was formed by heating the mixture at 100°C for 3 min and then at 65°C for 5 min, and finally by cooling down to room temperature. The 5'-phosphorylated oligonucleotide mixture (consisting of different mutagenic oligonucleotides in equal molarities) was annealed to the single-stranded gap of this duplex. The oligonucleotides used are shown in Table 1. After extension

and ligation, the DNA mixture was transformed into *E. coli* BMH71-18*mutS* (repair deficient). The supernatant was used to reinfect strain MK30-3 (*sup* mutant). Single-stranded DNA was isolated from colorless plaques, and the mutations were first identified by dot-blot hybridization by using the ^{32}P-labeled mutagenic oligonucleotide mixture as a probe. Increasing the stringency of the washes by raising the temperature stepwise discriminated between different mutations, because thermal stability of oligonucleotide DNA duplexes depends on the number of mismatched base pairs and on the type of mismatch (23). Routinely, 48 single-stranded DNAs were screened per round of mutagenesis, showing overall mutant yields between 40 and 60%. For the oligonucleotides VI and VII, not all of the expected mutations were found, which was probably a result of a nonmolar ratio of the oligonucleotides within these mixtures.

All mutations were finally confirmed by dideoxy-sequence analysis (46) with internal *CEN6* sequencing primers. The actual sequences of the mutations are shown in Fig. 2C. To facilitate the nomenclature of the various mutations, each nucleotide within CDEI and CDEIII was numbered (see Fig. 2B). The term CDEI(7-A) indicates that in CDEI nucleotide 7 from the left is changed to an A. The symbol ∇ means insertion, and Δ means deletion. In both cases, the numbers given in parentheses refer to the first and last nucleotide between which the insertion or deletion occurred. In the case of an insertion, the additional nucleotides are shown. For further cloning of the mutations, see below.

Plasmid constructions. The mutations created for this study by the M13 gapped duplex DNA approach were recloned into pUC18 for cloning purposes and into pJH1 to perform the mitotic stability assay. The universal sequencing primer was annealed to the single-stranded DNAs of M13 carrying the *CEN* mutations, and after the polymerase reaction, the 1.16-kb centromere-containing fragments were liberated by digestion with *Bam*HI and *Sal*I. These fragments were cloned into *Bam*HI-*Sal*I-cut pUC18 and into *Bam*HI-*Xho*I-cut pJH1. Thus, the 1.3-kb *CEN6* (wild-type) sequence of pJH1 was replaced with 1.16-kb DNA carrying the mutated *CEN* sequences.

The correspondence of the different point mutations (see Fig. 2C) and clones is as follows: CDEI(7-A), pUC18-*CEN6*:16; CDEI(7-C), pUC18-*CEN6*:17; CDEI(7-G), pUC 18-*CEN6*:18; CDEI(8-T), pUC18-*CEN6*:26, CDEI(8-A), pUC18-*CEN6*:27; CDEI(8-C), pUC18-*CEN6*:28; CDEIII(2-A,3-G), pUC18-*CEN6*:22; CDEIII(8-T), pUC18-*CEN6*:29; CDEIII(8-T,9-G), pUC18-*CEN6*:30; CDEIII(14-A), pUC18-*CEN6*:19; CDEIII(14-G), pUC18-*CEN6*:20; CDEIII(14-T), pUC18-*CEN6*:21; CDEIII(15-T), pUC18-*CEN6*:23; CDE III(15-A), pUC18-*CEN6*:24; and CDEIII(15-C), pUC18-*CEN6*:25.

In vitro-constructed *CEN6* mutants, which were produced earlier (17), were renamed and were also available as pUC derivatives (1.16-kb *Bam*HI-*Sal*I CEN fragment): CDE III(21-C) [*CEN6*(BglII), pUC9-*CEN6*:1]; CDEIII(21-C,19∇ 20-TA) [*CEN6*(BglII+2), pUC9-*CEN6*:2/5]; CDEIII(17Δ25) [*CEN6*(BglII-7), pUC9-*CEN6*:6]; CDEIII(19∇20-T) [*CEN6* (+T), pUC18-*CEN6*:10]; CDEIII(19∇20-G) [*CEN6*(+G), pUC18-*CEN6*:11].

The plasmid pJH1 was used to generate the mitotic stability data of the mutants. The construction of pJH1 and pJH2 has been described earlier (named pJH-CEN6 [wild type] in reference 17). In pJH2, which is used as a negative control, the centromeric region is deleted.

The parental plasmid used for constructing pYCF5 (yeast chromosome fragmentation) was pYCF3 (D. Vollrath, R. Davis, C. Connelly, and P. Hieter, Proc. Natl. Acad. Sci. USA, in press). A unique 2.7-kb *Eco*RI-*Hin*dIII DNA fragment derived from the left arm of chromosome III between the genetic markers *CEN3* and *LEU2* (region D8B; C. Newlon, unpublished results) was inserted into the *Eco*RI-*Hin*dIII sites of the polylinker of pYCF3. The resultant plasmid (pYCF5, see Fig. 3) is acentric and lacks a strong *ARS*. It therefore does not stably transform yeasts in circular form or when linearized at *Not*I. The features of pYCF5 make it suitable for testing the stabilities conferred by wild-type and mutant *CEN* sequences because only those plasmids which recombine in vivo with a homologous chromosomal target will have their markers stably propagated. *CEN6* and *CEN6** (mutant) fragments were inserted into pYCF5 as follows: 1.2-kb *Bam*HI-*Sal*I fragments from YRP14/ARS1/*CEN6*:2, pUC18-*CEN6*:10, pUC18-*CEN6*:11, pUC9-*CEN6*:6, pUC9-*CEN6*:1, pUC9-*CEN6*:2/5, and pUC18-*CEN6*:(16 through 30) were inserted into the *Bam*HI and *Sal*I site of pYCF5; 6.4-kb *Sal*I-*Bgl*II fragments from pJH10, pJH11, and pJH12 were inserted into the *Bam*HI and *Sal*I site of pYCF5.

Generation of wild-type and mutant centromere-containing chromosome fragments carrying the left arm of chromosome III. pYCF5/*CEN6** plasmids were linearized at the *Eco*RI or *Not*I site and transformed into YNN290 by the lithium acetate procedure (22), selecting Ura$^+$ transformants. For each plasmid construction, 16 independent transformants were streaked onto nonselective (YPD) plates. This verified a pink phenotype, resulting from one copy of the *SUP11* gene per diploid genome (18). Six independent isolates were prepared for electrophoresis as described previously (47), and the chromosome-sized DNA was then subjected to orthogonal field alternation gel electrophoresis (OFAGE) (5, 6) (14 h, 10°C, 275 V, and 38-s pulse frequency) to determine electrophoretic karyotypes.

Mobilities of the newly generated chromosome fragments were compared with those of previously characterized standards to determine whether recombination had occurred with the left arm of chromosome III. The standards were made using a pYCF5/*CEN6* (wild-type) plasmid. Restriction endonuclease digestion of pYCF5/*CEN6* (wild-type) plasmid with *Eco*RI creates a linear molecule which targets to the left arm of chromosome III when transformed into yeast cells. Digestion of the plasmid with both *Eco*RI and *Bam*HI targets the molecule to the right arm of chromosome VI. (The experimental details of chromosome fragmentation are as described by Hieter et al. [manuscript in preparation].) The DNA content of these standards was verified by probing Southern blots of OFAGE gels (19, 21) with labeled DNA (12) of cloned genes from the left arm of chromosome III (*LEU2*) or from the right arm of chromosome VI (*ACTI*). Since the mobility of a chromosome fragment carrying the left arm of chromosome III is distinct from a chromosome fragment carrying the right arm of chromosome VI (see Fig. 4), strains containing the correct chromosome III fragment were directly identified by comparing the OFAGE mobility with those of the standards.

Gene conversion of the *CEN6* mutations to wild type during pYCF5/*CEN6** integrative transformation (targeted to the left arm of chromosome III) seemed extremely unlikely (as described below in Results). Nevertheless, we rigorously demonstrated the presence of *CEN6* mutations on chromosome fragments in those strains that showed near-wild-type mitotic stability (YPH288, -289, -290, -295, and -297) as follows. Genomic DNA was prepared from each of the strains, digested with *Sal*I and *Eco*RI, electrophoresed

on 0.8% agarose gels, and blotted to nitrocellulose (49), and triplicate blots were probed separately with a 1.2-kb *CEN6* (wild-type) probe (as control) and two *CEN6* wild-type sequence 15-mer oligonucleotides, one spanning the left half of CDEIII (5'-AATAGTTTTTGTTTT-3') and the other spanning the right half of CDEIII (5'-AAGATGTAAAA TAGG-3'). YPH281 (carrying *CEN6* [wild-type] chromosome fragment) DNA was used as a control. Hybridizations were done at 29°C in 6× SSC (1× SSC is 0.15 M NaCl plus 0.015 M sodium citrate) and washed at 34°C in 6× SSC. Autoradiograms confirmed the presence of the *CEN6* mutations, as evidenced by the differential hybridization of the left-half or right-half oligonucleotide probes to *Sal*I-*Eco*RI restriction fragments containing mutant or wild-type *CEN6* DNA (data not shown).

Mitotic plasmid stability assay. This assay was performed as previously described (8, 41). All pJH plasmids carrying the various point mutations were transformed into yeast strain SX1-2. Transformants were restreaked onto minimal plates again. Six independent transformants were then chosen for the assay.

Determining loss rates of chromosome fragments carrying mutant *CEN* sequences by fluctuation analysis. For each mutant, a single pink colony (containing both parental copies of chromosome III with a chromosome fragment) was picked off a nonselective plate and grown for 4 to 6 h in minimal medium, selecting for the marked chromosome fragment. Cultures were diluted, mixed vigorously, and spread onto indicator plates (minimal medium with 6 μg of adenine per ml) at a density of 50 cells per plate (100 by 15 mm). Plates were incubated for 24 to 27 h at 30°C until small single colonies formed. Ten test colonies of equal size (determined by measuring the diameter under 10× magnification) were picked by using a Pasteur pipette to obtain the entire colony with a plug of agar. Plugged colonies were placed in minimal medium and disrupted to single cells by vortexing. Half of the suspension was distributed over the surfaces of five large indicator plates (150 by 15 mm), and the data obtained were multiplied by 2 to reflect the whole test colony. Strains with *CEN* mutations, causing chromosome fragment loss at a rate of $>10^{-2}$, required an additional manipulation to obtain adequate data for analysis. They were analyzed by picking 80 colonies, of which approximately 25% originated from cells with a single copy of the chromosome fragment. Ten percent of each resuspended colony was distributed over a single large indicator plate, and the data obtained for each of the chromosome-fragment-containing colonies were multiplied by 10 to reflect the whole colony. The total number of colonies obtained in each "plate out" indicates the number of cell divisions that had occurred during test colony growth, and the number of uniformly red colonies indicates the total number of cells that had lost the chromosome fragment prior to plating. The rate of loss per cell division was obtained by determining the median number of cells without the chromosome fragment for the 10 test colonies analyzed. This median value was used to determine the mean number of chromosome fragment loss events during the growth of the test colony, using the mathematical expression derived by Lea and Coulson (26). The mean number of loss events divided by the total number of cell divisions that had occurred during the colony growth is the rate of loss per cell division (see Fig. 1 for examples of data generation).

To determine the validity of counting red colonies and total colonies to determine loss rate, the growth rates of cells with one or zero copies of the chromosome fragment were determined to be equal (data not shown) by fluctuation analysis under conditions identical to those described above. We were unable to determine the rate of chromosome gain per cell division (i.e., generation of white colonies) because cells with two copies of the chromosome fragment have a slower growth rate.

YPH288 CDEIII (2-A,3-G)		
Test Colony	Colony Size	Red Segregants
1	60,900	247
2	64,800	125
3	58,800	112
4	62,500	92
5	61,100	75
6	73,800	57
7	55,400	37
8	65,400	20
9	65,300	15
10	64,800	12
Avg.	63,400	
Median		66
Mean		16.4
Chromosome fragment loss rate= 16.4/63,400= 2.58×10^{-4}		

YPH287 CDEI (8-C)		
Test Colony	Colony Size	Red Segregants
1	15,500	380
2	12,600	278
3	15,100	184
4	12,200	156
5	20,100	108
6	19,200	104
7	15,000	62
8	16,300	54
9	13,400	54
10	White colony picked	
Avg.	15,490	
Median		108
Mean		24.4
Chromosome fragment loss rate= 24.4/15,490 = 1.57×10^{-3}		

FIG. 1. Two examples of data generation for fluctuation analysis. The calculations followed the mathematical expressions developed by Lea and Coulson (26). Avg., Average.

RESULTS

In vitro-generated mutations in *CEN6* DNA. Figure 2A summarizes some features of *CEN* DNA. CDEI consists of a stretch of 8 nucleotides (uTCACuTG), which are fully conserved within all centromere DNAs analyzed to date. CDEIII is 25 bp long ($TGT^{T}_{A}T^{T}_{A}TG$..TTCCGAA.....AAA) and shows conserved and nonconserved nucleotides. In its center is a core sequence of 7 bp, and on the left of CDEIII are two additional G nucleotides, which are 100% conserved. Both CDEI and CDEIII exhibit palindromic structures covering one or two helical turns, respectively. All our studies were performed with the centromere DNA of chromosome VI (*CEN6*). The complete sequence of CDEI and CDEIII of *CEN6* is shown in Fig. 2B. To facilitate the discussion of the various point mutations, the nucleotides within CDEI and CDEIII were numbered from left to right.

All point mutations created in this study are shown in Fig. 2C. We selected our mutations to determine whether the degree of conservation of an individual base reflects its importance of centromere function and to assess the importance of the palindromic structures which may represent sites for protein binding. We decided to mutagenize the perfectly conserved right 2 bases of CDEI [positions 7 and 8 of CDEI, which are, respectively, CDEI(7) and CDEI(8)] (Fig. 2C). All possible changes were introduced by oligonucleotide-directed mutagenesis to assess whether the alteration of such preserved nucleotides (either by transition or transversion) would affect, to different degrees, the ability to form an active centromere. The conserved sequence of CDEIII contains five G · C base pairs, which are conserved in all *CEN* sequences analyzed so far; two are part of the palindrome, the other three are not. Because of their perfect conservation and their distribution in CDEIII, these G · C and C · G base pairs were our preferred targets for mutagenesis. We introduced all possible changes at positions 14 and

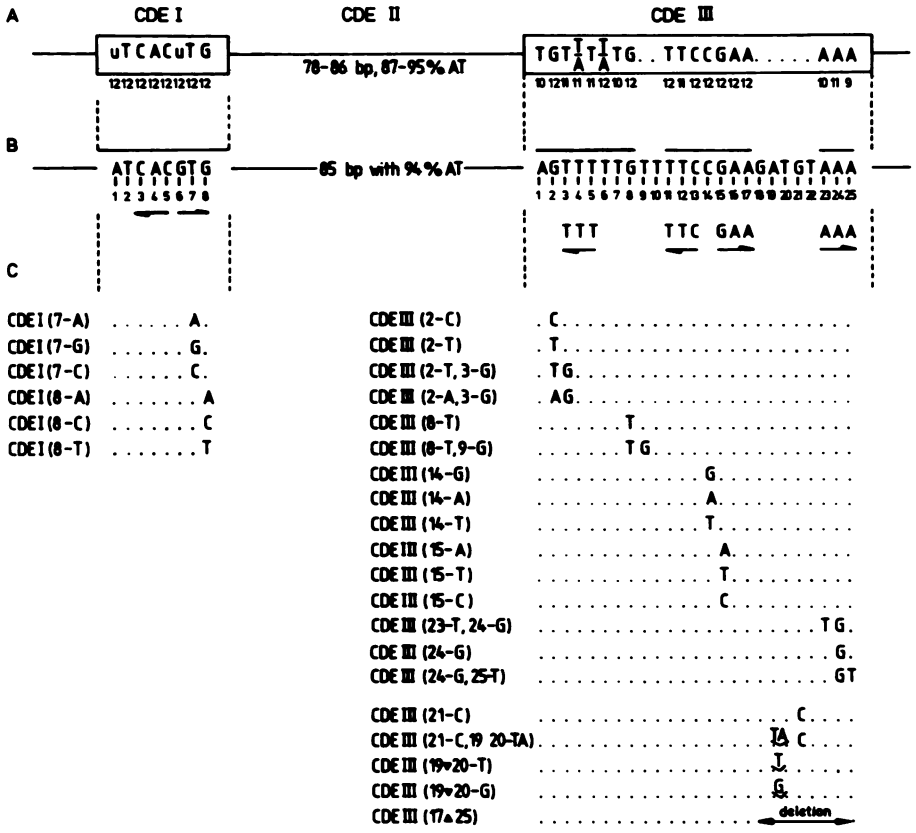

FIG. 2. DNA sequences of centromeres and centromere mutants. (A) Centromere consensus sequence, based on 12 *CEN* DNAs from *S. cerevisiae*. The numbers written below the bases indicate how many sequences out of the 12 carry this particular nucleotide (u = purine). By convention, only the upper strand is shown. (B) Centromere DNA sequence from chromosome VI. In this case, the numbers below the sequence define each nucleotide position within CDEI and CDEIII, to facilitate the nomenclature of the mutants (for details, see Materials and Methods). Below CDEI and CDEIII, the dyad symmetry is indicated. (C) Point mutations used in this study. Unchanged nucleotides are indicated by dots, and altered nucleotides are written out. For details of the mutagenesis work, see Materials and Methods. The five mutations at the bottom of the CDEIII mutation list (three with insertions, one with a deletion) were constructed earlier (17).

15 of CDEIII: the C · G base pair at position 14 forms the center of the 7-bp core palindrome, whereas the G · C base pair at position 15 is part of one half-site. Additionally, the two G · C base pairs at positions 2 and 8 of CDEIII were changed. Since it had been found before that space changes between conserved subregions at the right side of CDEIII lead to decreased *CEN* activities [e.g., CDEIII(19▽20-G); 17], shifts of the G · C base pairs were also introduced. The G · C base pair was moved from position 2 to position 3 and in another construction from position 8 to position 9. Previous work had shown (17) that the three A residues at the right end of CDEIII are important for *CEN* function, since deletion of this subregion yielded nonfunctional *CEN* mutations. Further point mutations in this part of the dyad were made to characterize this region in more detail.

Introduction of *CEN* DNA sequence mutations into yeast cells and in vivo testing. Commonly used assays to determine quantitatively the ability of a particular centromere DNA sequence to assemble into an active centromere are the mitotic plasmid stability assay (8, 18, 24), quantitative mating test (9), and loss of the chromosomal *URA3* marker by using 5′-fluoro-orotic acid (2, 54). Drawbacks associated with these methods include the high background loss rate of *CEN* plasmids, phenotypic lag or leakiness of the genetic marker being scored, and loss of markers due to mitotic recombination and gene conversion. We therefore developed and used a new assay and compared the results with those obtained by using the plasmid assay. We generated large (~150-kb) linear chromosomal fragments carrying the *URA3* gene as a genetic marker, the *SUP11* gene for measuring the mitotic stability of these artificial chromosomes, and the mutated *CEN* sequence of interest in the background of the diploid yeast strain YNN290, which is homozygous for *ade2-101*. Loss of the artificial chromosome during nonselective outgrowth can be monitored visually by the appearance of red sectors in the otherwise pink colonies (18).

To produce the chromosomal fragments, we constructed the plasmid pYCF5 (yeast chromosome fragmentation vector) (Fig. 3A). In addition to the *URA3*, *SUP11*, and *CEN6* mutant DNA, the vector contains a 1.5-kb *Bgl*II-HindIII fragment of the telomere-adjacent Y′ region (7) (herein called Y′a) and a 2.7-kb *Eco*RI-*Hin*dIII fragment (herein called D8B), which is about 10 kb left from *CEN3* (Newlon, unpublished results). Cleavage of the pYCF5/*CEN6* vectors with *Not*I or *Eco*RI creates a linear molecule with the Y′a sequence at one end and the D8B sequence at the other. Transformation of yeast cells with this small linear DNA gives rise to large linear chromosomal fragments because, upon two homologous recombination events, the Y′a region is "healed to" a telomere (11, 55) and the D8B region targets (37, 45) to the left arm of chromosome III, which is then

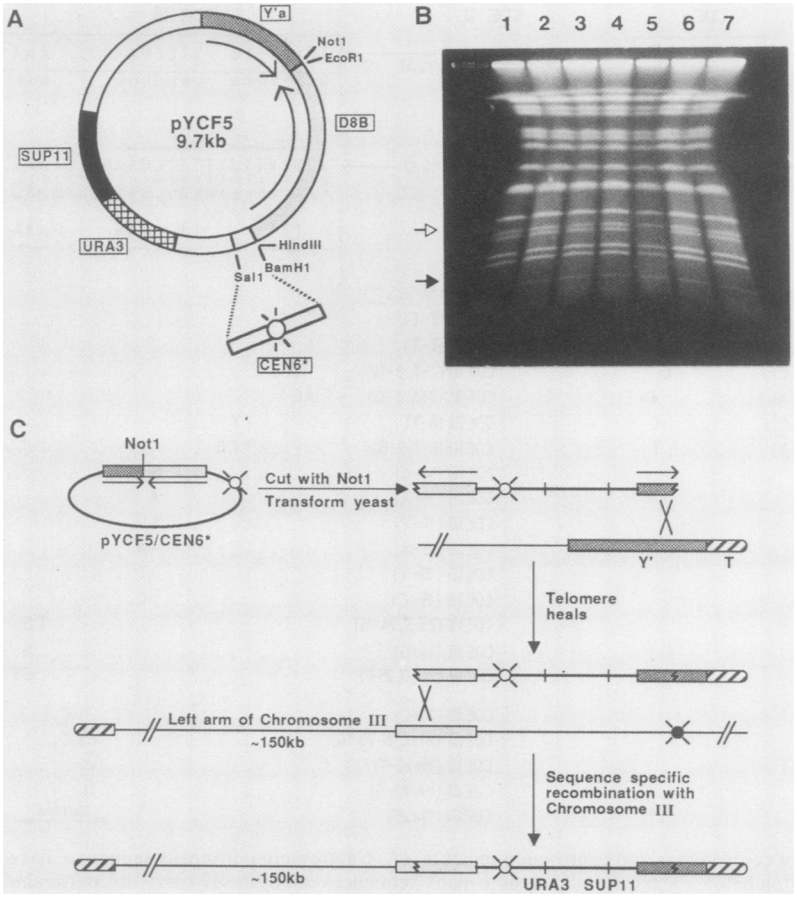

FIG. 3. Fragmentation vector for analyzing *CEN* DNA sequence mutants. A map of pYCF5 is shown with the unique restriction sites *Not*I, *Eco*RI, *Hin*dIII, *Bam*HI, and *Sal*I indicated. The vector contains *URA3* (for selecting transformants), *SUP11* (for monitoring mitotic stability of chromosome fragments generated by transformation), Y′ sequences (for efficient conversion of one end of the transformed DNA to a telomere), and a unique DNA sequence (from the left arm of chromosome III, named D8B) for in vivo addition of almost the entire left arm of chromosome III to the transformed DNA. Mutant or wild-type *CEN6* DNA was inserted into the *Sal*I-*Bam*HI (shown) or *Hin*dIII-*Bam*HI (not shown). (B) OFAGE analysis of the chromosome fragments generated by transformation of linearized plasmids. For each *CEN6* DNA mutant, six independent transformants were analyzed for the presence of the chromosome fragment. Lane 1 shows the electrophoretic karyotype of the parent yeast strain YNN290. The diploid strain is heterozygous for a chromosome III-length polymorphism (open arrow), which allows one to visualize the fate of the chromosome III homolog with which the pYCF5/*CEN* vector recombines. Lanes 2 through 7 show six independent transformants generated in a typical transformation experiment. Clearly visible are the newly created chromosome III fragments (solid arrow), which show a length of approximately 150 kb. In about 10% of the transformants, the generation of the telocentric chromosome fragment was accompanied by the loss of one of the parental chromosome III homologs (lane 5) representing the karyotype $2n-1+CF$. Fluctuation analysis for determining the rate of mitotic chromosome loss was always performed with $2n+CF$ strains (e.g., lane 2). (C) Scheme for the in vivo generation for mutant *CEN6*-containing chromosome fragments. pYCF5 (mutant or wild-type) plasmid DNA was linearized with *Eco*RI or *Not*I and transformed into the diploid yeast strain YNN290, selecting for Ura^+. One end of the linear plasmid molecule contains sequences (Y′a) that are efficiently repaired to a functional telomere; the other end contains a unique DNA sequence (D8B), whose normal genomic position is found on the left arm of chromosome III. Approximately 50% of the URA^+ transformants possess the approximately 150-kb new chromosome shown at the bottom, in which all of the chromosome III sequences distal to the unique sequence D8B have been added. Note that the genetic marker (*SUP11*) used to score chromosome fragment loss is located on the short arm embedded in pBR322 sequence. Since this chromosome arm has no homolog, loss of *SUP11* cannot occur by mitotic crossing over. The presence of a wild-type *CEN6* sequence in the vector portion yields a stable chromosome fragment with a rate of chromosome loss per cell division of 2×10^{-4}.

completely copied onto the vector. The result of these recombination events is the appearance of a 150-kb-long telocentric chromosomal fragment and a strain trisomic for most of the left arm of chromosome III. We chose a chromosome III left arm fragmentation scheme for two reasons. First, left arm chromosome III aneuploidy is tolerated in our strains with no detectable deleterious effects (data not shown). Second, at a low frequency, one of the parental chromosome III homologs is lost during transformation, yielding a mating-competent diploid transformant, because the strain becomes monosomic for the right arm of chromosome III, which contains the mating-type locus. Such $2n-1+CF$ (CF = chromosome fragment) transformants arise approximately 10% of the time (P. Hieter, unpublished results). These mating diploid strains will be useful in future *CEN* mutant suppressor experiments.

The in vivo generation of the chromosomal fragments is shown schematically in Fig. 3C. Upon transformation and restreaking of the transformants, pink and red colonies are obtained (see Materials and Methods). Approximately 50%

of the Ura$^+$ transformants carry a chromosome fragment. As the diploid yeast strain YNN290 used for this work is homozygous for the *ade2* ochre mutation and the copy number of the SUP11 gene determines the phenotype of the yeast cell (18), these transformants form all pink colonies with red sectors. The amount of sectoring depends on the type of *CEN* sequence located on the chromosome fragment. The other 50% of the transformants are red and contain the recircularized plasmid, which is rapidly lost under nonselective conditions, since it carries only a weak *ARS3* (which is linked to the *SUP11* gene). To verify that the newly created telocentric chromosomal fragments contained the expected DNA, independent isolates of the transformation were analyzed for their electrophoretic karyotype by OFAGE. The analysis of six independent transformants of one transformation is presented (Fig. 3B). The parental yeast strain (lane 1) exhibited a polymorphism for length for chromosome III (open arrow) that enabled us to distinguish between recombination events leading to the karyotype $2n-1+CF$ or $2n+CF$. Transformants of the karyotype $2n-1+CF$ (lane 5) were obtained 14 times in the 160 transformants analyzed by OFAGE in this study; the others were of the type $2n+CF$ (e.g., lane 2). The solid arrow at the bottom indicates the position of the newly generated chromosome fragment.

The telocentric chromosome fragments carrying the various *CEN* mutations exhibit very low frequencies of mitotic gene conversion to wild-type *CEN* DNA via a gene conversion or double crossover with homologous DNA. This was never observed in the present study. The low frequency of reversion is presumably a result of the presence of nonhomologous sequences flanking the 1.2-kb *CEN6* DNA (Fig. 3C). Furthermore, loss of the *URA3* and *SUP11* markers from the chromosome fragment by mitotic recombination is not possible or extremely rare, because the markers are positioned on the short arm of the chromosome fragment. This pBR322-derived arm does not recombine, as it lacks a genomic counterpart. Gene conversion (there are eight tRNA^{Tyr} genes in the genome) or other complex rearrangements leading to a Sup11$^-$ (red) phenotype also do not occur at a significant rate. This was demonstrated by isolating a red segregant from each of 26 independent, pink colonies containing a *CEN6* (wild-type) chromosome fragment. All 26 Sup11$^-$ strains were simultaneously *ura* mutants and none of the strains contained rearrangements, as evidenced by probing Southern blots of OFAGE gels with sequences unique to the chromosome fragment long arm. Therefore, loss of the *SUP11* gene is due solely to chromosome loss events, rather than to the sum of loss events due to chromosome loss and recombination. All mitotic stability analyses were performed on transformants containing both parental copies of chromosome III plus the chromosome fragment ($2n+CF$) (i.e., identical to the transformant analyzed in lane 2 of Fig. 3B). We thus excluded possible differences in loss rates due to gene dosage differences on chromosome III.

Transformants with undesired chromosome fragments due to mistargeting of the transformed linear DNA. For certain *CEN* mutants that yielded very high loss rates on plasmids, we could never detect chromosome III-derived telocentric fragments. Instead, we found in some cases rare recombinant chromosome fragments containing the right arm of chromosome VI. Although other models are possible, these events can be explained by proposing a degradation model, which implies that the free ends of the linearized plasmid pYCF5/*CEN6* are degraded when transformed into yeast cells (Fig. 4). If degradation of the free end containing unique DNA from chromosome III occurs, the chromosomal target

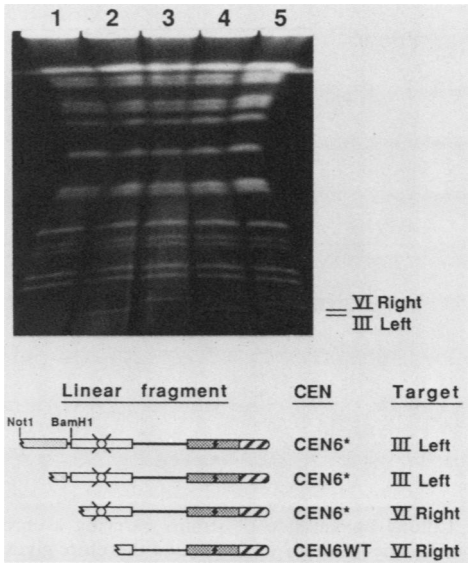

FIG. 4. Targeting of the linear pYCF5/*CEN6* to different chromosomal locations. One model to explain the rare recombination events that generate chromosome fragments containing the right arm of chromosome VI proposes degradation of the free ends of the linear plasmid pYCF5/*CEN6* when transformed into yeast cells, as indicated at the bottom of the figure. Shown on top is the OFAGE analysis of different targeting events. Lane 1 shows the OFAGE karyotype of the parent yeast strain. Lanes 2 and 3 show the different mobilities of chromosome fragments generated by linearizing the vector with *Not*I, which targets the unique end of the vector to chromosome III (lane 2), or by linearizing the vector with *Not*I and *Bam*HI, which targets the unique end to chromosome VI (lane 3). Lanes 4 and 5 show representatives of the two possible karyotypes found as a result of transformation of a *Not*I-linearized pYCF5/*CEN6* plasmid; lane 4 shows generation of a chromosome III fragment, whereas lane 5 shows the generation of a chromosome VI fragment, possibly due to degradation of the transformed vector into the chromosome VI homology before recombination with the genomic host target could occur. Note the different sizes of the chromosome III and VI fragments, which make it possible to detect chromosome VI-derived fragments by ethidium-stained OFAGE gels. A representation of the proposed degradation of DNA from the unique end of the linear vector and resultant recombination products is shown at the bottom. When the unique end consists of sequences from chromosome III, the resultant chromosome fragment carries the left arm of chromosome III and the mutant *CEN6*. Degradation into *CEN6* sequences targets the recombination instead to the right arm of chromosome VI. If degradation takes place past the mutation in the *CEN6* DNA, the resultant chromosome fragment will carry a wide-type *CEN6* sequence.

of the plasmid may change. If the degradation goes past the *CEN6* mutation, a chromosome fragment is generated that carries the wild-type *CEN6* plus the right arm of chromosome VI. When linear pYCF5/*CEN6** molecules harboring a mutation which abolishes *CEN* function were transformed into yeast cells, the only stable transformants we obtained were those which regenerated wild-type *CEN* sequences by the above scenario. This was seen with the mutations CDEIII(21-C,19∇20-AT), CDEIII(14-A), CDEIII(14-T), and CDEIII(14-G). The electrophoretic karyotypes of strains carrying chromosome fragments which resulted from targeting of the linear pYCF5/*CEN6* to different chromosomal locations are presented (Fig. 4). First, we constructed standard strains carrying telocentric fragments derived from chromosome III or VI by digesting pYCF5/*CEN6* (wild type), either with *Not*I or with *Not*I and *Bam*HI and trans-

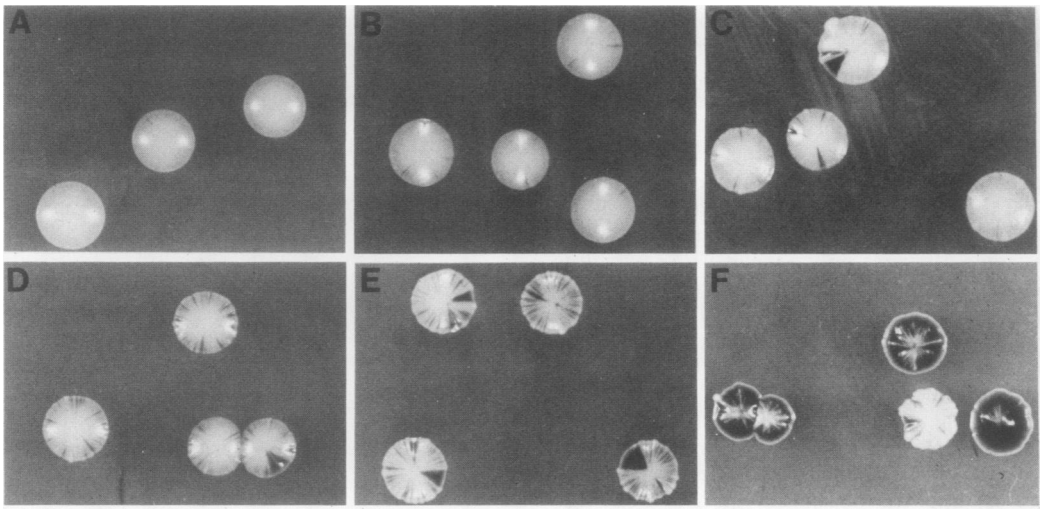

FIG. 5. Colony appearance of strains carrying a chromosome fragment with wild-type or mutant *CEN6*. The parent yeast strain is homozygous for the *ade2-101* mutation and therefore gives rise to red colonies. (A) Transformation with a linearized pYCF5/*CEN6* wild-type vector yields mitotically stable *SUP11*-marked chromosome fragments. Transformed strains generate homogeneously pink colonies, which show, on average, less than one visible red sector per colony. The estimated loss rate of this telocentric chromosome is 1.9×10^{-4}. Panels B through F show increased rates of loss of the chromosomal fragment due to mutations within the *CEN6* sequence, as evidenced by an increased red sectoring phenotype. Qualitatively, two- to threefold differences can be seen. Specifically, the loss rates of the chromosomal fragment were as follows: 5.2×10^{-4} for CDEI(7-G) (panel B), 8.3×10^{-4} for CDEI(8-A) (panel C), 1.5×10^{-3} for CDEIII(19∇20-T) (panel D), 3.8×10^{-3} for CDEIII(19∇20-G) (panel E), and 3.7×10^{-2} for CDEIII(17Δ25) (panel F).

forming into yeast cells. The resulting chromosome fragments contained either the left arm of chromosome III (lane 2) or the right arm of chromosome VI (lane 3). Southern blots verified the DNA content (data not shown). Since the mobilities of these two telocentric fragments are different, strains containing the correct chromosome III fragment were directly identified by comparing the OFAGE mobility with the standard strains described above. Lanes 4 and 5 show two transformants derived from transformation with a *Not*I-digested pYCF5/*CEN6**. Lane 4 shows the fragment carrying chromosome III DNA, whereas the fragment in lane 5 can be identified as having been derived from chromosome VI. Our analysis showed that when the left arm of chromosome III was present, all (100%) independent isolates of a given mutation had the same phenotype. Therefore, we can preclude the possibility that a *CEN6* mutant is converted to wild type during integrative transformation by choosing transformants that have been targeted to chromosome III, rather than to chromosome VI. Nevertheless, we formally excluded this possibility by analyzing those *CEN* mutations exhibiting wild-type behavior with oligonucleotide probes against restriction digests of genomic DNA (see Materials and Methods).

Mitotic chromosome and plasmid loss rates of various *CEN6* mutations. A total of 23 different point mutations were introduced into the *CEN6* sequence, and their effects on mitotic *CEN* function were analyzed both on chromosome fragments and, for comparison, on plasmids. Three additional point mutations were tested only on plasmids.

To obtain chromosome fragment loss rates, the various *CEN6* point mutants were cloned into pYCF5 (see Materials and Methods for details) and the linearized pYCF5/*CEN6** plasmids were transformed into the diploid yeast strain YNN290. When the transformants were restreaked onto nonselective plates, the colony color phenotype of each particular *CEN* mutant showed up clearly (Fig. 5). As little as two- to threefold differences in loss rates were already visible at this point. The appearance of the correct chromosome fragment was monitored by OFAGE as described above. For each mutation, one transformant of the karyotype $2n+CF$ was then selected to determine the mitotic chromosome fragment loss per cell division by fluctuation analysis (method of the median [26]). Two examples of data generation are shown in Fig. 1. The data for chromosome fragment loss rates per cell division for all *CEN* DNA sequence mutants, as well as for the two wild-type centromeres from chromosomes IV and VI, are compiled in Table 2. It has previously been shown that replacement of the centromere from chromosome III by the *CEN* sequence of chromosome XI has no measurable effect on chromosome distribution during mitosis (9), indicating clearly that yeast centromeres are not chromosome specific. We verified this observation by analyzing the mitotic stability of chromosome fragments carrying *CEN6* or *CEN4*. The loss rates are almost identical, 1.87×10^{-4} for *CEN6* and 1.68×10^{-4} for *CEN4*. The loss rates for the wild-type *CEN* sequences of about 2×10^{-4} allow us to express the quantitative effects of important nucleotide positions within the *CEN6* DNA over a range of 3 orders of magnitude (10^{-1} to 10^{-4}), whereas the plasmid assay offers a range of only 1 order of magnitude (10^{-1} to 10^{-2}).

For comparison, each of the *CEN6* mutations was analyzed on circular plasmids. Figure 6 summarizes the plasmid mitotic stability data. The plasmid pJH1 (10.3 kb) contains 4.5 kb of original *CEN6* DNA and the *TRP1* gene for selecting transformants. A 1.3-kb *Bam*HI-*Xho*I *CEN6* (wild-type) DNA fragment was replaced by the 1.16-kb *Bam*HI-*Sal*I fragment bearing the various *CEN6* point mutations embedded in original *CEN6* surrounding DNA. The various pJH constructions carrying the point mutations were then transformed into the haploid yeast SX1-2. Trp^+ transformants were colony purified, and single colonies were subjected to mitotic stability tests. By growing the transformants for 10 generations in nonselective medium and subsequent replica plating, the number of cells which still harbored the particular pJH plasmid was determined. In

TABLE 2. Loss rates per mitotic cell division determined by the chromosome fragment stability assay[a]

Yeast strain	Mutation	Rate of chromosome fragment loss/cell division
YPH281	*CEN6* (wild type)	1.9×10^{-4}
YPH186	*CEN4* (wild type)	1.7×10^{-4}
YPH282	CDEI(7-A)	5.0×10^{-4}
YPH283	CDEI(7-C)	3.2×10^{-4}
YPH284	CDEI(7-G)	5.2×10^{-4}
YPH285	CDEI(8-T)	4.3×10^{-4}
YPH286	CDEI(8-A)	8.3×10^{-4}
YPH287	CDEI(8-C)	1.6×10^{-3}
YPH288	CDEIII(2-A,3-G)	2.6×10^{-4}
YPH289	CDEIII(8-T)	1.9×10^{-4}
YPH290	CDEIII(8-T,9-G)	3.1×10^{-4}
	CDEIII(14-A)	No CEN function
	CDEIII(14-G)	No CEN function
	CDEIII(14-T)	No CEN function
YPH291	CDEIII(15-T)	4.2×10^{-2}
YPH292	CDEIII(15-A)	7.3×10^{-2}
YPH293	CDEIII(15-C)	7.9×10^{-2}
YPH294	CDEIII(23-T,24-G)	4.6×10^{-4}
YPH295	CDEIII(24-G)	2.2×10^{-4}
YPH296	CDEIII(24-G,25-T)	4.1×10^{-4}
YPH297	CDEIII(21-C)	4.0×10^{-4}
	CDEIII(21-C,19∇20-TA)	No CEN function
YPH298	CDEIII(19∇20-T)	1.5×10^{-3}
YPH299	CDEIII(19∇20-G)	3.8×10^{-3}
YPH300	CDEIII(17Δ25)	3.7×10^{-2}

[a] Chromosome fragment data were obtained by performing fluctuation analyses by the method of the median (26) on strains carrying a chromosome fragment with the *CEN* constructions shown. The desired chromosome III-derived chromosome fragments were not recovered from transformations using vectors carrying mutations which abolished *CEN* function, and therefore these mutations are shown as having no *CEN* function.

almost all cases, six independent transformants were tested (the actual number of each mutant is given in parentheses) and the average percentage of plasmid-containing cells was calculated, together with the standard deviation (Fig. 6). As in previous publications (17, 40), we express the effects of centromere mutants when tested on plasmids as percentages of cells carrying the plasmid after 0 and 10 generations of nonselective growth.

(i) Mitotic *CEN* activity reduced by point mutations in CDEI. All eight nucleotides in CDEI are 100% conserved among all 12 sequenced centromere DNAs. Therefore, it seemed likely that any change of these bases would impair *CEN* function. Indeed, all point mutations we introduced gave rise to reduced centromere activity when tested both on plasmids and on chromosome fragments (Table 2 and Fig. 6). All possible base changes at position 7 of CDEI have slightly less severe effects than alterations at position 8 [e.g., a 3-fold-higher chromosome fragment loss rate for CDEI(7-G) compared with a 10-fold-higher loss rate for CDEI(8-C)]. This is observed on plasmids, as well as on chromosome fragments. The CDEI(8) results were already striking when the 0 generation data were obtained in the plasmid assay (Fig. 6B). Of the six mutations tested in CDEI, the transversion from wild-type G · C to C · G [CDEI(8-C)] shows the most negative influence on *CEN* function.

(ii) Importance of conserved subregions revealed by scattered mutagenesis of CDEIII. To determine whether all conserved subregions in CDEIII are important or essential for a fully active mitotic centromere, we introduced point mutations in all conserved nucleotide blocks. At the same time, these modifications also altered the half-sites of the palindrome.

We initially focused on the core of CDEIII. Introduction of all possible point mutations at position 15 [CDEIII(15)] severely reduces centromere activity. The chromosome fragment loss rates for these three *CEN* point mutations (Table 2) were 100-fold increased compared with that of the wild type. The plasmid data were consistent with these results; even at 0 generations, the number of cells bearing the plasmid was quite low (around 10%). We conclude that position 15 is very important for proper *CEN* function. This G · C base pair is part of the inner dyad of CDEIII and is therefore likely to be involved in protein binding. In contrast, the adjacent C · G base pair at position 14 [CDE III(14)] is not part of the palindrome. However, all three base-pair changes demonstrate that this position is critical for mitotic centromere function. At 0 generations in the plasmid assay, all three point mutations, CDEIII(14-A), CDEIII(14-G), and CDEIII(14-T), showed behavior identical to that of the negative-control pJH2, which contains no *CEN* DNA. Additionally, we were never able to generate stabilized chromosome fragments derived from chromosome III by using these mutations. Instead, only the rare chromosome VI-derived telocentric chromosome fragments were detected, which all showed *CEN* (wild-type) activity (see above and Fig. 4).

The triple A region (positions 23 through 25), which is also part of the dyad at the right end of CDEIII, has previously been shown to be involved in *CEN* function using a plasmid assay (17). We now introduced one single-base-pair change, CDEIII(24-G), and two double-base-pair changes, CDE III(23-T,24-G) and CDEIII(24-G,25-T), in this subregion. The *CEN* activity for the double mutants was only slightly reduced (about twofold on the chromosome fragment), and the *CEN* activity of the point mutation CDEIII(24-G) was close, if not identical, to that of the wild type. We have shown earlier that space changes at the right side of CDEIII result in strongly affected or abolished *CEN* function (17) when tested on plasmids. These pJD constructs were now quantitatively analyzed in our chromosome fragment colony color assay. The introduction of 1 bp [CDEIII(19∇20-T) and CDEIII(19∇20-G)] between the core and the triple A region of CDEIII led to a 10-fold increase in chromosome loss rate. Introduction of 2 bp [CDEIII(19∇20-TA)] at the same position abolished *CEN* function. Change of 1 bp within this region, CDEIII(21-C), had a small effect on *CEN* function when tested on the chromosome fragment (twofold-increased loss), even though the spacing was maintained. These results indicate that the sequence content of this nonconserved subregion is of importance for *CEN* function.

On the left side of CDEIII, there are two purine G · C base pairs, CDEIII(2) and CDEIII(8), which are 100% conserved. Surprisingly, all point mutations introduced at these positions caused only minor reductions in *CEN* activity (1.5- to 2-fold on the chromosome fragment). The mutations which move the original G · C base pair one position closer to the core of CDEIII, CDEIII(2-A,3-G) and CDEIII(8-T,9-G), had a similar effect.

DISCUSSION

In the present study, a large number of single- and double-base-pair substitutions were introduced into the conserved centromere DNA elements I and III of *CEN6* DNA to determine the functional domains of the centromere DNA. In addition, we wanted to generate, if possible, a collection

A.

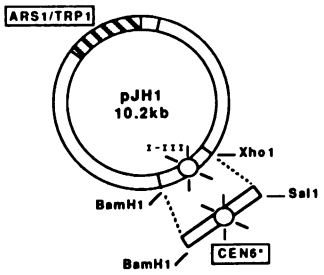

B.

Plasmid	Type of Mutation	% of Trp+ cells after growth in nonselective medium		
		0 gen	10 gen	
pJH 1	wt	88 ± 7	75 ± 7	(6)
pJH13	CDEI (7-A)	87 ± 4	60 ± 5	(6)
pJH14	CDEI (7-C)	87 ± 4	62 ± 6	(6)
pJH15	CDEI (7-G)	84 ± 1	48 ± 6	(5)
pJH23	CDEI (8-T)	81 ± 4	51 ± 7	(6)
pJH24	CDEI (8-A)	58 ± 20	13 ± 12	(6)
pJH25	CDEI (8-C)	58 ± 6	16 ± 4	(6)
pJH29	CDEIII (2-C)	81 ± 4	67 ± 4	(4)
pJH30	CDEIII (2-T)	86 ± 6	77 ± 16	(5)
pJH31	CDEIII (2-T,3-G)	86 ± 5	62 ± 5	(5)
pJH19	CDEIII (2-A,3-G)	88 ± 7	68 ± 4	(6)
pJH26	CDEIII (8-T)	85 ± 5	70 ± 5	(6)
pJH27	CDEIII (8-T,9-G)	87 ± 3	67 ± 7	(6)
pJH16	CDEIII (14-A)	2 ± 1	0	(6)
PJH17	CDEIII (14-G)	2 ± 1	1 ± 1	(6)
pJH18	CDEIII (14-T)	3 ± 1	3 ± 1	(5)
pJH20	CDEIII (15-T)	10 ± 5	1 ± 1	(6)
pJH21	CDEIII (15-A)	9 ± 3	2 ± 1	(6)
pJH22	CDEIII (15-C)	9 ± 12	3 ± 3	(5)
pJH12	CDEIII (23-T,24-G)	84 ± 8	64 ± 6	(4)
pJH10	CDEIII (24-G)	88 ± 2	71 ± 2	(6)
pJH11	CDEIII (24-G,25-T)	86 ± 3	65 ± 6	(5)
pJH2	----------	3 ± 1	1 ± 1	(6)

FIG. 6. Mitotic plasmid stability assay. (A) Map of pJH1 plasmid (17), which was used to determine the plasmid mitotic stability of the *CEN* mutants. The *ARS* sequence allows autonomous replication of the plasmid in yeast cells, while *TRP1* is used to select transformants and as a marker to measure the percentage of cells carrying the plasmid with the mutated centromere. The 1.3-kb *Bam*HI-*Xho*I DNA fragment carrying *CEN6* (wild type) was replaced by a 1.17-kb *Bam*HI-*Sal*I fragment carrying the particular *CEN* mutants. For details of the cloning, see Materials and Methods. The location and the orientation of CDEI, CDEII, and CDEIII are indicated. (B) Results of the plasmid assay. SX1-2 was transformed with the various pJH-*CEN* plasmids. Transformants were restreaked onto selective plates. For each mutation, six independent transformants were usually taken and grown nonselectively for 10 generations. The cultures were diluted and plated on nonselective plates to yield 100 to 200 colonies per plate. The percentage of Trp^+ colonies was determined by replica plating on selective medium. For the 0 generation determination, the cells were plated out directly without outgrowth. The percentages of TRP^+ colonies, together with the standard deviation and, in parentheses, the number of transformants tested, are given. The plasmid pJH2 lacks the centromere sequence and therefore shows the typical segregation bias of an *ARS* plasmid.

of *CEN* mutants with intermediate centromere activity reductions for use in reversion studies.

The centromere mutations were analyzed when located on plasmids and on chromosome fragments. Although the mitotic plasmid stability assay has proved useful in our hands (18, 41), this assay is not suited to quantitate small centromere activity reductions because of the high basal level of instability (10^{-2}) associated with wild-type *CEN* plasmids. For this reason, and to circumvent drawbacks of other chromosome-based centromere assays, we developed a new assay using *SUP11*-marked chromosome fragments. This method enabled us to accurately quantitate the effects of these mutations on mitotic centromere function. The sectoring pattern of the colonies often allowed us to immediately order the effects of *CEN* mutants, since two- to threefold differences in chromosome fragment loss rates could easily be recognized (Fig. 5). For a rigorous quantitation of the effects of *CEN* DNA sequence mutations, we performed fluctuation analysis by using the chromosome fragment color assay. In principle, the *CEN*-linked genetic information (*URA3* and *SUP11*) can be used in two ways. At first, we intended to determine the frequencies of chromosome loss events in independent cultures by using the positive selection system for Ura^- mutants by plating on 5′-fluoro-orotic acid plates (2). Unfortunately, we encountered the problem of leakiness in the drug selection. After plating the colonies on 5′-fluoro-orotic acid, we found the number of Ura^- colonies to be too high. Viewing the plates under the microscope revealed, in addition to the visible colonies, many arrested microcolonies (up to 100 cells), indicating phenotypic lag for 5′-fluoro-orotic acid sensitivity. Any chromosome fragment loss event that had occurred after plating during additional cell divisions would lead to an Ura^- colony and an overestimation of the frequency of Ura^- segregants in the culture at the time of plating. We therefore decided to perform the fluctuation analysis by measuring the loss of *SUP11*, instead of *URA3*. Cells were put on plates with limiting amounts of adenine and subsequently scored for total pink ($2n$+CF) and red ($2n$) colonies. Although this required a large number of plates, neither leakiness in selection nor phenotypic lag was a problem, since only entirely red colonies were counted (i.e., colonies derived from single cells that had lost the chromosome fragment prior to plating). In addition, all-red segregants (26 of 26 tested) were shown to be due to loss of the chromosome fragment (i.e., chromosome loss event); none were due to a recombination event. Finally, when the desired chromosome III-derived chromosome fragment was verified by OFAGE analysis, all of the transformants exhibited the same colony phenotype (i.e., gene conversion of the *CEN6* mutation to wild type did not occur during transformation, since integrative recombination was targeted to chromosome III, rather than VI).

The loss rate (1.7×10^{-4} to 1.9×10^{-4}) of the 150-kb chromosome fragment carrying a wild-type centromere sequence (*CEN4* or *CEN6*) was significantly higher than that reported for a full-length wild-type chromosome (2×10^{-5} [16]). However, as similar loss rates (1.2×10^{-4}) have been reported for deletion derivatives of chromosome III, which are 120 and 150 kb in length (53), a possible explanation for the difference in stability might be the relatively small size of our artificial chromosome. Alternatively, the fact that the telomere and the centromere are less than 8 kb apart or the presence of unknown stabilizing or destabilizing factors on the right or left arms of chromosome III (53) might play a role.

Sequence comparison of the 12 cloned *CEN* DNAs led to a centromere consensus sequence (Fig. 2A). The functional left- and right-hand boundaries of the centromere 6 DNA sequence have been identified by deletion analysis (17, 40). Recently, we have succeeded in cloning a 125-bp DNA fragment carrying the *CEN6* DNA sequence and an additional 6 bp left from CDEI and 1 bp right from CDEIII. The plasmid and the chromosome fragment loss rates of this "minimal length" *CEN6* sequence show wild-type centromere activity, indicating that the boundaries of the conserved centromere elements correspond to the functional

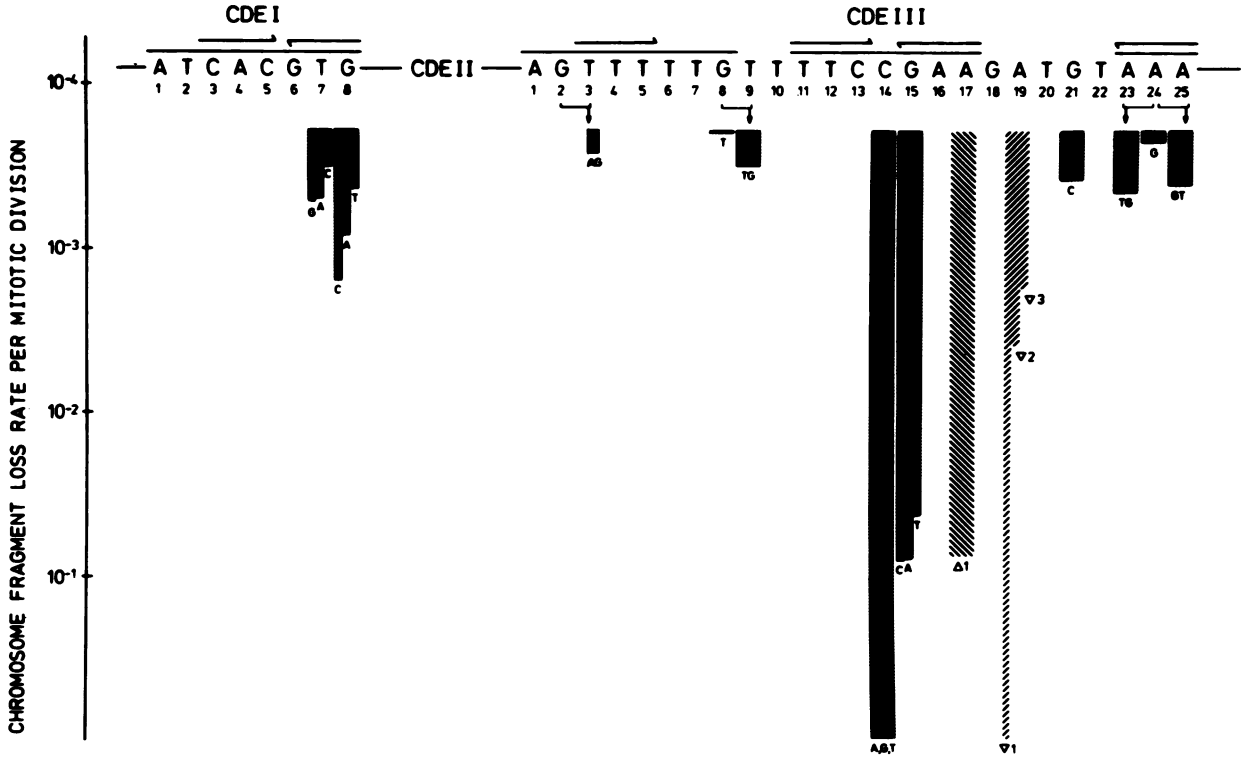

FIG. 7. Schematic representation of chromosome fragment loss rates for the *CEN6* mutations generated in this study. At the top of the figure, the DNA sequences of CDEI and CDEIII are shown, with the conserved nucleotides and the dyad structures indicated by horizontal lines and half arrows, respectively. To facilitate the identification of the various point mutants, all nucleotides have been numbered (see Materials and Methods). The dark vertical bars represent the loss rates per cell division of the chromosome fragments bearing the various point mutations (in Table 2). Each bar depicts one or more mutants generated at one specific position in CDEI or CDEIII. The nucleotide(s) which replace the wild-type nucleotide(s) are indicated below the bars. Double-base-pair changes are marked by brackets. The striped vertical bars represent the various deletion or insertion mutants. Symbols: Δ1, CDEIII(17Δ25); ∇1, CDEIII(21-C,19∇20-TA); ∇2, CDEIII(19∇20-G); ∇3, CDEIII(19∇20-T).

boundaries of the centromere region (Cottarel et al., manuscript in preparation). This result makes an involvement of sequences outside of CDEI and CDEIII very unlikely. However, the possibility still exists that foreign DNA surrounding the *CEN* DNA can influence centromere function in a negative way.

Importance of conserved nucleotides for mitotic centromere function. One question we wanted to address with our mutational analysis was whether the change of a totally conserved base pair within CDEI and III would always lead to a decrease in mitotic centromere activity and whether this decrease would be of a similar order of magnitude. Surprisingly, every point mutation we introduced at perfectly conserved nucleotide positions did not lead to a drastic impairment of *CEN* function (Fig. 7). The magnitude of the effects covered the whole spectrum of possible centromere activity reductions. While the mutation CDEIII(8-T) had essentially no effect on *CEN* function, all single-base-pair changes at position 14 of CDEIII abolished *CEN* activity. Between these two extremes were point mutations with 2- to 3-fold- [CDEI(7)], 10-fold- [CDEI(8-C)], and 100-fold- [CDEIII(15)] higher loss rates. These results clearly show that the degree of conservation (100%) as such is no indication for a corresponding importance of these base pairs in mitotic centromere function. It remains to be seen whether meiotic centromere function is affected by any of the point mutations.

We report here, for the first time, point mutations in CDEI (Fig. 7). Single-base-pair changes at positions 7 and 8 in CDEI have distinct consequences in affecting centromere function, showing 2- to 10-fold-higher chromosome fragment loss rates. In both cases, a transversion showed the most severe effect on *CEN* activity. CDEI(8) seems to be more important than CDEI(7). Since we have not analyzed all eight positions of CDEI, we cannot exclude the possibility that other nucleotides within this element play a superior or subordinate role compared with nucleotides at positions 7 and 8.

The centromere DNA element III consists of conserved subregions which form a palindromic sequence. Our mutagenesis study shows that of the three conserved subregions only nucleotides within the highly conserved central core (positions 11 through 17) are critical for *CEN* function [CDEIII(14) and CDEIII(15)]. Single- and double-base-pair changes in the other conserved subregions or in the nonconserved space between the subregions have very little effect. For example, the single-base-pair changes CDEIII(8-T) and CDEIII(2-T) showed centromere activity close to that of the wild type, even though the G · C base pairs at these positions were completely conserved in all *CEN* DNAs analyzed. These data are in accordance with mutational studies on *CEN3* DNA (30, 35), in which the G · C base pair at CDEIII(8) was changed to an A · T base pair and was found to exhibit nearly wild-type *CEN* activity when placed on chromosome III. Furthermore, when we introduced point mutations at the right end of the palindrome of CDEIII at positions 23 through 25, again only small increases in loss

rates were observed. These results indicate that the core sequence of CDEIII (which is the center of the palindrome) is of essential importance for centromere function. Dyad symmetries in procaryotes have been shown to be important, since some regulatory sites of this type are recognized by dimers of the cognate DNA-binding protein (38). In yeast cells, it was shown that the regulatory site of *HIS3*, to which the positive regulatory protein *GCN4* binds, consists of a 9-bp dyad interrupted by 1 bp (20). We find for *CEN6* that the C · G base pair in the center of the CDEIII dyad [CDEIII(14)] is of fundamental importance and that all three possible nucleotide replacements abolish *CEN* function. In contrast, base pair changes of the wild-type G · C base pair at CDEIII(15), which belongs to the right half of the palindrome, show some residual activity. We conclude that the central C · G base pair is essential for centromere function and may be part of one half-site of the dyad, implying that CDEIII consists of two nonidentical recognition sites for two (nonidentical?) or more protein subunits. This is also indicated by the observation that the palindrome does not lie in a symmetrical position within the 25-bp-long CDEIII.

Recently, similar results were obtained for the centromere of chromosome III (30, 35; also see Addendum). McGrew et al. (30) introduced two C · G to T · A transitions at positions 13 and 14 of CDEIII by using the sodium bisulfite mutagenesis method. The base-pair change at CDEIII(14) abolished *CEN* function when tested on a plasmid. The point mutation at CDEIII(13) also had a dramatic effect on centromere activity; when substituted for the centromere on chromosome III, the stability of the altered chromosome III was reduced by 3 orders of magnitude (30). These results are now confirmed and extended by our data on *CEN6*. Position 15 in CDEIII was also analyzed by McGrew et al. (30) (G · C to A · T), as well as by Ng et al. (35) (G · C to A · T and G · C to C · G), with conflicting results. In our tests, all possible nucleotide replacements at this position led to an increased rate (up to 400-fold) of chromosomal loss per cell division when quantitated on the chromosome fragment (in accordance with Ng et al. [35]). A possible explanation for the conflicting result (30) is that the CDEIII(8-A) mutation was converted to wild type during one-step gene replacement transformation.

The palindrome of CDEIII exhibits, at its right end, a triple A region (position 23 through 25), which seemed to be essential for *CEN* function, since deletion of two of the three A residues led to an inactive *CEN* in the mitotic plasmid test (17). Our point mutations CDEIII(24-G), CDEIII(23-T,24-G), and CDEIII(24-G,25-T) only showed maximally twofold-higher loss rates on the chromosome fragment. Ng et al. (35) found that transversion from an A · T base pair to a C · G base pair at position 24 in *CEN3* led to a 10-fold increase in their estimate of loss rate, and the double-base-pair change A · T A · T to T · A C · G led to a 250-fold increase in their estimate of loss rate. Viewing the 12 *CEN* DNAs sequenced so far shows that, for some centromeres, T · A base pairs were found within the triple A region (*CEN7*, *-10*, *-13*, and *-15*); only *CEN1* exhibited a C · G base pair at position 23. This, and the mutagenesis results, indicate that although some variability is tolerated, the primary sequence of the triple A region does contribute to centromere function.

In conclusion, the present study verifies the importance of the centromere DNA elements CDEI and CDEIII as primary sequence determinants of mitotic centromere function. Single- and double-base-pair changes within both elements affected centromere efficiency, suggesting an interaction between *CEN* DNA and *CEN* DNA-binding proteins. The point mutations within CDEI clearly verify the participation of this element in centromere function. The point mutations and insertions in CDEIII reveal the importance of both the sequence and spacing of the conserved subregions that form an interrupted palindrome. The assay used in this study allows us to quantitate loss rates per cell division of chromosome fragments bearing the various *CEN* mutants without the drawbacks of other systems. In addition, this assay, together with our mutant collection, will enable us to start a screen for second-site revertants.

ACKNOWLEDGMENTS

We thank W. Bannwarth (Hoffmann-LaRoche Inc.) for the synthesis of the oligonucleotides VI and VII; R. D. Pridmore for kind help in preparing some of the *CEN6* mutants; Carol Newlon for providing us with the cloned D8B DNA fragment; Shellie Hamilton for expert work in preparing the manuscript; and Bertha Robinson, Quentin Burley, and Grace Harrison for their technical support.

J.H.H. thanks the Deutsche Forschungsgemeinschaft (Bonn, Federal Republic of Germany) for a postdoctoral fellowship during his stay at the Biocenter in Basel, where most of the mutants were constructed. This work was supported by Public Health Service grant 5P01CA16519-13 from the National Institutes of Health and by Pew Scholars grant 86-909GHE to P.H. and by grant 3.334-0.82 from the Swiss National Foundation for Scientific Research and by a grant from the Deutsche Forschungsgemeinschaft to P.P.

ADDENDUM

Two mutational analyses of *CEN* DNA function have recently appeared. R. Ng and J. Carbon (Mol. Cell. Biol. **7**:4522–4534, 1987) analyzed the effects of four point mutations and three deletion mutations in CDEIII on mitotic *CEN* function and presented evidence for the existence of a CDEIII-binding protein in cell extracts. S. Cumberledge and J. Carbon (Genetics **117**:203–212, 1987) demonstrated the importance of CDEI, both in mitotic and meiotic *CEN* function, by constructing and analyzing deletion mutations in CDEI. The results presented here are in agreement with these reports. In addition, M. Saunders, M. Fitzgerald-Hayes, and K. Bloom (Proc. Natl. Acad. Sci. USA **85**:175–179, 1988) analyzed the effects of mutationally altered *CEN* DNA on chromatin structure surrounding the centromere region. The results correlated the presence of the nuclease-protected core with centromere function.

LITERATURE CITED

1. **Bloom, K., and J. Carbon.** 1982. Yeast centromere DNA is in a unique and highly ordered structure in chromosomes and small circular minichromosomes. Cell **29**:305–317.
2. **Boeke, J., F. Lacroute, and G. Fink.** 1984. A positive selection for mutants lacking orotidine-5'-phosphate decarboxylase activity in yeast: 5-fluoro-orotic acid resistance. Mol. Gen. Genet. **197**:345–346.
3. **Bram, R. J., and R. D. Kornberg.** 1987. Isolation of a *Saccharomyces cerevisiae* centromere DNA-binding protein, its human homolog, and its possible role as a transcription factor. Mol. Cell. Biol. **7**:403–409.
4. **Carbon, J., and L. Clarke.** 1984. Structural and functional analysis of a yeast centromere (CEN3). J. Cell Sci. Suppl. **1**:43–58.
5. **Carle, G., and M. Olson.** 1984. Separation of chromosomal DNA molecules from yeast by orthogonal-field-alternation gel electrophoresis. Nucleic Acids Res. **12**:5647–5664.
6. **Carle, G., and M. Olson.** 1985. An electrophoretic karyotype for yeast. Proc. Natl. Acad. Sci. USA **82**:3756–3760.
7. **Chan, C., and B. Tye.** 1983. Organization of DNA sequences

and replication origins at yeast telomeres. Cell **33**:563–573.
8. **Clarke, L., and J. Carbon.** 1980. Isolation of a yeast centromere and construction of functional small circular chromosomes. Nature (London) **287**:504–509.
9. **Clarke, L., and J. Carbon.** 1983. Genomic substitutions of centromeres in *Saccharomyces cerevisiae*. Nature (London) **305**:23–28.
10. **Davis, R., D. Botstein, and J. Roth.** 1980. Advanced bacterial genetics. Cold Spring Harbor Laboratory, Cold Spring Harbor, N.Y.
11. **Dunn, B., P. Szauter, M. Pardue, and J. Szostak.** 1984. Transfer of yeast telomeres to linear plasmids by recombination. Cell **39**:191–201.
12. **Feinberg, A., and B. Vogelstein.** 1983. A technique for radio labelling DNA restriction fragments to high specific activity. Anal. Biochem. **132**:6–13.
13. **Fitzgerald-Hayes, M., L. Clarke, and J. Carbon.** 1982. Nucleotide sequence comparisons and functional analysis of yeast centromere DNAs. Cell **29**:235–244.
14. **Fritz, H., R. Belagaje, E. Brown, R. Fritz, R. Jones, G. Lees, and H. Khorana.** 1978. High pressure liquid chromatography in polynucleotide synthesis. Biochemistry **17**:1257–1267.
15. **Gaudet, A., and M. Fitzgerald-Hayes.** 1987. Alterations in the adenine-plus-thymine-rich region of *CEN3* affect centromere function in *Saccharomyces cerevisiae*. Mol. Cell. Biol. **7**:68–75.
16. **Hartwell, L., S. Dutcher, J. Wood, and B. Garvik.** 1982. The fidelity of mitotic chromosome reproduction in *S. cerevisiae*. Recent Adv. Yeast Mol. Biol. **1**:28–38.
17. **Hegemann, J., R. Pridmore, R. Schneider, and P. Philippsen.** 1986. Mutations in the right boundary of *Saccharomyces cerevisiae* centromere 6 lead to nonfunctional or partially functional centromeres. Mol. Gen. Genet. **205**:305–311.
18. **Hieter, P., C. Mann, M. Snyder, and R. Davis.** 1985. Mitotic stability of yeast chromosomes: a colony color assay that measures nondisjunction and chromosome loss. Cell **40**:381–392.
19. **Hieter, P., D. Pridmore, J. Hegemann, M. Thomas, R. Davis, and P. Philippsen.** 1985. Functional selection and analysis of yeast centromeric DNA. Cell **42**:913–921.
20. **Hill, D., I. Hope, J. Macke, and K. Struhl.** 1986. Saturation mutagenesis of the yeast *his3* regulatory site: requirements for transcriptional induction and for binding by GCN4 activator protein. Science **234**:451–457.
21. **Huberman, J., R. Pridmore, D. Jaeger, B. Zonneveld, and P. Philippsen.** 1986. Centromeric DNA from Saccharomyces uvarum is functional in Saccharomyces cerevisiae. Chromosoma **94**:162–168.
22. **Ito, H., Y. Fukuda, K. Murata, and A. Kimura.** 1983. Transformation of intact cells treated with alkali cations. J. Bacteriol. **153**:163–168.
23. **Ikuta, S., K. Takagi, R. Wallace, and K. Itakura.** 1987. Dissociation kinetics of 19 base paired oligonucleotide-DNA duplexes containing different single mismatched base pairs. Nucleic Acids Res. **15**:797–811.
24. **Koshland, D., J. Kent, and L. Hartwell.** 1985. Genetic analysis of the mitotic transmission of minichromosomes. Cell **40**:393–403.
25. **Kramer, W., V. Drutsa, H. Jansen, B. Kramer, M. Pflugfelder, and H.-J. Fritz.** 1984. The gapped duplex DNA approach to oligonucleotide directed mutation construction. Nucleic Acids Res. **12**:9441–9456.
26. **Lea, D., and C. Coulson.** 1949. The distribution of numbers of mutants in bacterial populations. J. Genet. **49**:264–285.
27. **Mandel, M., and A. Higa.** 1970. Calcium-dependent bacteriophage DNA infection. J. Mol. Biol. **53**:159–162.
28. **Maniatis, T., E. F. Fritsch, and J. Sambrook.** 1982. Molecular cloning: a laboratory manual. Cold Spring Harbor Laboratory, Cold Spring Harbor, New York.
29. **Mann, C., and R. W. Davis.** 1986. Structure and sequence of the centromeric DNA of chromosome 4 in *Saccharomyces cerevisiae*. Mol. Cell. Biol. **6**:241–245.
30. **McGrew, J., B. Diehl, and M. Fitzgerald-Hayes.** 1986. Single base-pair mutations in centromere element III cause aberrant chromosome segregation in *Saccharomyces cerevisiae*. Mol. Cell. Biol. **6**:530–538.
31. **Messing, J., and J. Vieira.** 1982. A new pair of M13 vectors for selecting either strand of double-digest restriction fragments. Gene **19**:269–276.
32. **Murray, A., N. Schultes, and J. Szostak.** 1986. Chromosome length controls mitotic chromosome segregation in yeast. Cell **45**:529–536.
33. **Murray, A., and J. Szostak.** 1983. Construction of artificial chromosomes in yeast. Nature (London) **305**:189–193.
34. **Murray, A., and J. Szostak.** 1985. Chromosome segregation in mitosis and meiosis. Annu. Rev. Cell. Biol. **1**:289–315.
35. **Ng, R., S. Cumberledge, and J. Carbon.** 1986. Structure and function of centromeres, p. 225–239. *In* J. Hicks (ed.), Yeast cell biology. Alan R. Liss, Inc., New York.
36. **Norrander, J., T. Kempe, and J. Messing.** 1983. Improved M13 vectors using oligonucleotide-directed mutagenesis. Gene **19**:101–106.
37. **Orr-Weaver, T., J. Szostak, and R. Rothstein.** 1981. Yeast transformation: a model system for the study of recombination. Proc. Natl. Acad. Sci. USA **78**:6354–6358.
38. **Pabo, C., and R. Sauer.** 1984. Protein-DNA recognition. Annu. Rev. Biochem. **53**:293–321.
39. **Panzeri, L., I. Groth-Clausen, J. Shepherd, A. Stotz, and P. Philippsen.** 1985. Centromeric DNA in yeast. Chromosomes Today **8**:46–58.
40. **Panzeri, L., L. Landonio, A. Stotz, and P. Philippsen.** 1985. Role of conserved sequence elements in yeast centromere DNA. EMBO J. **4**:1867–1874.
41. **Panzeri, L., and P. Philippsen.** 1982. Centromeric DNA from chromosome VI in *S. cerevisiae*. EMBO J. **1**:1605–1611.
42. **Peterson, J., and H. Ris.** 1976. Electron microscopic study of the spindle and the chromosome movement in the yeast *S. cerevisiae*. J. Cell Sci. **22**:219–242.
43. **Ris, H., and P. Witt.** 1981. Structure of the mammalian kinetochore. Chromosoma **82**:153–170.
44. **Roman, H.** 1959. Studies of gene mutations in *Saccharomyces cerevisiae*. Cold Spring Harbor Symp. Quant. Biol. **21**:175.
45. **Rothstein, R.** 1983. One-step gene disruption in yeast. Methods Enzymol. **101**:202–211.
46. **Sanger, F., S. Nicklen, and A. R. Coulson.** 1977. DNA sequencing with chain-terminating inhibitors. Proc. Natl. Acad. Sci. USA **74**:5463–5467.
47. **Schwartz, D., and C. Cantor.** 1984. Separation of yeast chromosome-sized DNAs by pulsed field gradient gel electrophoresis. Cell **37**:67–75.
48. **Sherman, F., G. Fink, and C. Lawrence.** 1979. Methods in yeast genetics. Cold Spring Harbor Laboratory, Cold Spring Harbor, N.Y.
49. **Southern, E.** 1975. Detection of sequences among DNA fragments separated by gel electrophoresis. J. Mol. Biol. **98**:503–517.
50. **Struhl, K., D. Stinchcomb, S. Scherer, and R. Davis.** 1979. High-frequency transformation of yeast: autonomous replication of hybrid DNA molecules. Proc. Natl. Acad. Sci. USA **76**:1035–1039./
51. **Stinchcomb, D., C. Mann, and R. Davis.** 1982. Centromeric DNA from *Saccharomyces cerevisiae*. J. Mol. Biol. **158**:157–179.
52. **Stinchcomb, D., K. Struhl, and R. Davis.** 1979. Isolation and characterization of a yeast chromosomal replicator. Nature (London) **282**:39–43.
53. **Surosky, R., C. Newlon, and B. Tye.** 1986. The mitotic stability of deletion derivatives of chromosome III in yeast. Proc. Natl. Acad. Sci. USA **83**:414–418.
54. **Surosky, R., and B. Tye.** 1985. Construction of telocentric chromosomes in *Saccharomyces cerevisiae*. Proc. Natl. Acad. Sci. USA **82**:2106–2110.
55. **Szostak, J., and E. Blackburn.** 1982. Cloning yeast telomeres on linear plasmid vectors. Cell **29**:245–255.